JMEPEG (2003) 12:261-271 

# Non-Isothermal Annealing of a Cold Rolled Commercial Twin Roll Cast 3003 Aluminum Alloy

*E.S. Puchi-Cabrera, C.J. Villalobos-Gutiérrez, A. Carrillo, and F. Di Simone*

*(Submitted 6 February 2003)*

**It is shown that the recrystallization behavior of a cold rolled twin roll cast, commercial 3003 aluminum alloy under non-isothermal conditions, can be satisfactorily modeled by combining the approaches developed by Semiatin et al. and Puchi et al. The first approach allows the determination of the apparent activation energy for recrystallization without any ambiguity, information that can then be used in the second approach to define clearly the search range for the value of the apparent activation energy for recrystallization and to determine simultaneously the Avrami constants, from experiments conducted at a single heating rate. It is also shown that the apparent activation energy for recrystallization in this alloy varies between approximately 34 and 79 kJ/mol, with the trend being to find smaller values of this parameter as the strain applied to the material increases. Such low values of this energy were corroborated by isothermal experiments conducted in samples of the same material. The microstructural evolution of the samples annealed under non-isothermal conditions indicates that the rate of growth of the recrystallized grains in the rolling direction is significantly higher that in the short transverse direction, due to the pinning effect of the second phase particles aligned along the rolling direction, which leads to recrystallized structures with an aspect ratio significantly higher than 1. The effect of the strain applied to the material on the recrystallization kinetics is quantified by expressing the time required to achieve a given recrystallized fraction as a function of the effective strain, by a simple parametric relationship that involves three numerical constants. Recrystallization experiments conducted under non-isothermal conditions are found to be more suitable for the evaluation of the effect of the strain applied on the recrystallization kinetics in comparison with isothermal tests, since larger strains can be applied to material before the annealing treatment.**

**Keywords** 3003 aluminum alloy, non-isothermal annealing, recrystallization, twin roll cast

## 1. Introduction

Commercial twin roll cast 3003 aluminum alloys are usually cold rolled, after strip casting, from an initial thickness of approximately of 6 mm to 0.67 mm in four passes. To restore the ductility of the material after this primary stage of rolling, the rolled stock is subsequently annealed in a $CO_2$-$N_2$ atmosphere at a temperature of approximately 793 K for 8-10 h. However, for a coil of 8 ton in weight, the annealing treatment is conducted under non-isothermal conditions, which gives rise to a marked interaction between the recrystallization of the deformed matrix and the precipitation of fine particles that occurs due to the decomposition of the supersaturated alloy. The description of the change in the volume fraction recrystallized with annealing time under non-isothermal conditions can be carried out by a modified form of the classic Johnson-Mehl-Avrami-Kolmogorov equation (JMAK), as it has been previously reported by Puchi et al.[1,2] and Semiatin et al.[3]

**E.S. Puchi-Cabrera, C.J. Villalobos-Gutiérrez, A. Carrillo,** and **F. Di Simone,** School of Metallurgical Engineering and Materials Science, Faculty of Engineering, Universidad Central de Venezuela, Apartado Postal 47885 Los Chaguaramos, Caracas 1045, Venezuela. Contact e-mail: epuchi@reacciun.ve.

Puchi and co-workers[1,2] investigated the restoration and recrystallization kinetics of two twin-roll cast (TRC) and cold rolled commercial aluminum alloys, subsequently annealed under non-isothermal conditions. For such a purpose, the JMAK equation was generalized to take into account the continuous increase in temperature during annealing. In their investigations, samples of both commercial-purity aluminum and Al-1% Mn alloy were cold rolled and annealed non-isothermally.

The commercial-purity material was heated starting from room temperature up to 675 K at a heating rate of approximately 0.01 K/s. Once this temperature was achieved, it was maintained for 2 h such that the annealing cycle was completed in 12 h. During the annealing treatment groups of samples were removed from the furnace at every hour and subsequently water quenched. However, to study the restoration process in more detail, between the $8^{th}$ and $9^{th}$ hour the samples were extracted every 5-10 min.

For the 3003 alloy, the as-cast samples were previously homogenized at 793 K for 48 h and furnace cooled. Subsequently, these samples were cold rolled to two different thickness reductions, with and without reverting the rolling direction in every pass and annealed non-isothermally from room temperature up to 653 K in a period of 10 h. This final temperature was maintained for 6 more hours and groups of samples were removed from the furnace and water quenched every hour during the annealing treatment.

According to the authors, the description of the restoration curves determined for both alloys was observed to be quite satisfactory, particularly for the restoration data determined

from tensile strength measurements. An interesting result of these investigations was that for the 3003 alloy, the reversion of the rolling direction during processing led to an apparent homogenization of the strain applied and to a reduction of the stored energy in the material, in comparison with the samples in which the rolling direction was not reverted.

On the other hand, Semiatin and co-workers[3] developed a theoretical analysis for the description of the recrystallization kinetics during continuous heat treatment operations, by investigating such kinetics during very rapid heat treatments involving induction or direct-resistance heating. The applicability of the results derived from their model was established using continuous, rapid recrystallization data for a cold-worked low carbon steel and commercial-purity Ti. In both cases, the start and completion of the recrystallization process was determined as a function of the heating rate, which involved the rapid heating of samples to various peak temperatures at different rates and subsequent water quenching. Such data allowed the determination of the constants involved in the JMAK equation as well as the apparent activation energy for recrystallization.

The models advanced by Puchi et al.[1,2] and Semiatin et al.[3] can be used in a combined manner to determine, from a single set of data obtained at a constant heating rate, both the apparent activation energy for recrystallization and the Avrami constants involved in the formulation. Therefore, the present investigation has been conducted to study, by employing these two models, the recrystallization behavior under non-isothermal conditions, of a cold rolled commercial TRC 3003 alloy that has also been deformed to different thickness reductions. In this way, it has been possible to derive a simple parametric relationship capable of describing the effect of the strain applied to the material on the recrystallization kinetics during this kind of annealing.

### 1.1 Models Used in the Description of the Recrystallization Kinetics Under Non-Isothermal Conditions

The analysis conducted by Semiatin et al.[3] starts from an expression of the JMAK equation of the form:

$$X = 1 - \exp\left\{(-\ln 2)\left(\frac{t}{t_{0.5}}\right)^n\right\} \quad \text{(Eq 1)}$$

where X represents the volume fraction recrystallized, t the time, $t_{0.5}$ the time to achieve 50% recrystallization, and n the Avrami exponent. Thus, by assuming that $t_{0.5}$ in the previous equation typically follows an Arrhenius dependence on temperature, these authors concluded that for non-isothermal recrystallization processes, the volume fraction recrystallized could be expressed as a function of temperature and heating rate as:

$$\{-\ln(1 - \mathbf{X_f})\}^{1/n} = \frac{BR}{\dot{\theta} Q_r}\left\{T_f^2 \exp\left(-\frac{Q_r}{RT_f}\right)\right\} \quad \text{(Eq 2)}$$

where $Q_r$ represents the apparent activation energy for recrystallization, R the Universal gas constant, $\dot{\theta}$ the heating rate, B a numerical constant, $T_f$ any temperature above the initial annealing temperature, and $X_f$ the volume fraction recrystallized achieved at this temperature.

However, this approach has been criticized by Erukhimovitch and Baram[4] on the basis that the theoretical development of Semiatin et al.[3] relies on an expression for the JMAK equation (Eq 1), which is correct only when nucleation occurs in the entire volume. Thus, according to Erukhimovitch and Baram,[4] in most cases the nucleation in a recrystallization process is characterized by specific geometrical features and therefore, the activated sites at the onset of recrystallization are located either at grain boundaries and grain edges. Also, according to these authors and following the results of the work conducted by Henderson[5] on the applicability of the Avrami rate equation to non-isothermal transformation processes, the procedure followed by Semiatin et al.[3] can be used only under some specific restrictions which involved the dependence of the growth rate of the recrystallized material solely on temperature and not explicitly on time, the independence of the transformation rate on thermal history, and the occurrence of random nucleation at disperse second-phase particles. Such restrictions would limit the applicability of the JMAK formalism only to site-saturation transformations in which the nucleation stage takes place at the beginning of the process.

Following the work conducted by Cahn[6,7] and Matusita et al.,[8] these authors proposed that the description of the volume fraction recrystallized as a function of temperature in non-isothermal site saturation transformations, X(T), could be carried out by an equation of the form:

$$\ln[1 - X(T)] = \frac{C}{\alpha^n}\exp\left[-\frac{1.052nE}{RT}\right] \quad \text{(Eq 3)}$$

where $\alpha$ represents the constant heating rate, C a numerical constant, n the Avrami exponent, and E the activation energy for growth.

Semiatin et al.[9] in a subsequent communication have discussed the criticisms made by Erukhimovitch and Baram[4] on the basis of the applicability and limitations in using isothermal Avrami kinetics for the description of non-isothermal kinetics, a comparison between Eq 2 and 3, and the validity of Eq 2 for the description of non-isothermal kinetics. In addition, Semiatin et al.[9] demonstrated that the use of Eq 2 yielded similar results to those obtained by applying classic staircase calculations for several hypothetical non-isothermal recrystallization problems.

## 2. Experimental Techniques

The present investigation has been carried out employing samples of a commercial twin roll cast aluminum 1% manganese alloy (AA3003) provided by Aluminios de Carabobo S.A. (ALUCASA), Guacara, Edo. Carabobo, Venezuela, with the following composition (wt.%): 1.08 Mn, 0.63 Fe, 0.22 Si, 0.12 Cu, 0.016 Ti, and balance Al. The material was provided as strips of approximately 6.32 mm thickness. Specimens for cold rolling were machined maintaining the longest dimension parallel to the strip casting direction.

Some evaluations were also conducted directly in plant, particularly to assess the change in temperature as a function of annealing time of a coil of the same alloy heat treated after cold rolling. Such a semi-finished product had an external diameter of approximately 1500 mm, an internal diameter of about 520 mm, and a width of 1000 mm. The annealing process was carried out in a Guinea furnace (Spain) at a temperature of 793 K and controlled atmosphere. The coil was maintained inside the furnace for about 11 h and the temperature-time profile was determined by two thermocouples located at 5 and 320 mm from the steel mandrel at the center of the coil.

The cold rolling step was carried out at experimental level employing a 50 ton capacity, two-high, reversible, experimental rolling mill (Stanat, USA), with rolls of approximately 175 mm diameter at a peripheral speed of 67 mm/s. A first set of samples was cold rolled to 50, 70, and 90% thickness reduction, changing continuously the rolling direction. Tensile specimens were subsequently machined from the rolling stock and annealed non-isothermally in air from 298-778 K during 10 h at a constant heating rate, then maintained at 778 K for 4 h, and air cooled. Groups of samples were removed periodically from the annealing furnace and quenched in water to retain the high temperature microstructure.

A second set of samples was also cold rolled to 50% thickness reduction, from which tensile specimens were machined and annealed isothermally in a salt bath furnace at temperatures of 623, 673, and 723 K for different time periods ranging between approximately 5 and 48 000 s. Tensile tests were conducted on a computer-controlled servohydraulic machine (Instron 8502, Instron Corp., Canton, MA) at a crosshead speed of 0.05 mm/s. At least three samples were tested for every annealing condition. All the metallographic analyses were performed on the plane defined by the short transverse and the rolling directions.

Optical metallography was conducted under conditions of polarized light by electroetching the specimens in a solution of 52 mL hydrochloric acid (48%) and 973 mL distilled water, employing a stainless steel cathode and a potential of 22 V. Scanning electron microscopy (SEM) studies were conducted on a Hitachi S-2400 (Hitachi, Ltd., Tokyo, Japan) scanning microscope equipped with a Kevex-IV (Kevex X-Ray, Inc., Scotts Valley, CA) x-ray energy dispersive spectroscope unit.

## 3. Results and Discussion

The basic features of the initial microstructure of the as-cast samples used in this investigation are essentially the same as those reported by Olguín-Sandoval and Puchi-Cabrera[10] who also conducted recrystallization experiments with this alloy, but at a constant temperature. As shown in Fig. 1, under the optical microscope the material presents a characteristic columnar structure, which grows at approximately 45° from the surface to the centerline of the coil. Figure 1(a) shows that both columnar structures meet at the central plane of the sheet, whose interception with the cross section under examination is usually known as the "segregation line." The arrow on the picture indicates the roll casting direction, whereas the direction normal to the arrow represents the short transverse direction (ST).

Figure 1(b), on the other hand, illustrates that the grains near the edges appear to be more elongated than those at the center and a progressive change in their orientation from the surface to the center occurs. At this latter location the microstructure is observed to follow the roll casting direction. It is well known that during the solidification stage of a TRC process, a dynamic transition of the cast material into a subsequent hot-working condition takes place, which gives rise to a complex microstructure typical of the alloys processed by this route, which shows the predominance of higher cooling rates and more severe deformation near the edges, leading to a more elongated grain structure at such regions.

By SEM techniques, it was possible to establish the presence of many second phase particles both on the grain boundaries and also distributed along the matrix, whose size and composition vary throughout the cross section of the sheet. Thus, at the center it is common to observe dendrite-like morphology particles rich in Mn, Fe, and Si. On the other hand, near the edges, only small, elongated particles are usually present.

Figure 2 illustrates the results of the temperature-time profiles measured directly in the 3003 coil during the annealing industrial practice. Thus, it can be observed that after approximately 11 h of annealing the material close to the surface of the coil achieves a temperature of about 730 K, whereas in the locations closer to the steel mandrel the temperature is approximately 720 K. Therefore, once the coil is introduced into the industrial furnace, the outer parts of it start to heat up by radiation and convection, and the heat is subsequently conducted towards the center at a significant rate due to the relatively elevated thermal conductivity of the material, maintaining a relatively small difference between the surface and the center of the coil.

Figure 2 also illustrates that the heating rate found in the industrial annealing practice of this kind of semi-finished product is not constant but decreases as the temperature of the coil increases. Due to the large mass of the coil, the furnace temperature is not achieved after 11 h of treatment, remaining a difference of approximately 60-70 K between such a temperature and that of the alloy. However, the situation could also vary depending on the location of the coil inside the furnace, since within it there is always a small temperature gradient.

At laboratory scale, the annealing response of the material after cold rolling was first evaluated by means of the definition of a restoration index in the usual manner, determined from the changes in mechanical properties with annealing time. Such an index has been defined assuming the validity of a linear law of mixtures based on the equal strain distribution model between the restored and unrestored fractions present during annealing after cold rolling:

$$X_R = \frac{S_0 - S_i}{S_0 - S_f} \quad \text{(Eq 4)}$$

Therefore, the partially restored material is considered equivalent to a massive two-phase aggregate composed of a "soft" (restored) and a "hard" (unrestored) fractions whose mechanical strength can be determined from the mechanical properties of both fractions following such a simple law of mixtures. Thus, $S_0$ represents the ultimate tensile strength (UTS) of the material measured in the as-deformed condition, $S_i$ the UTS at

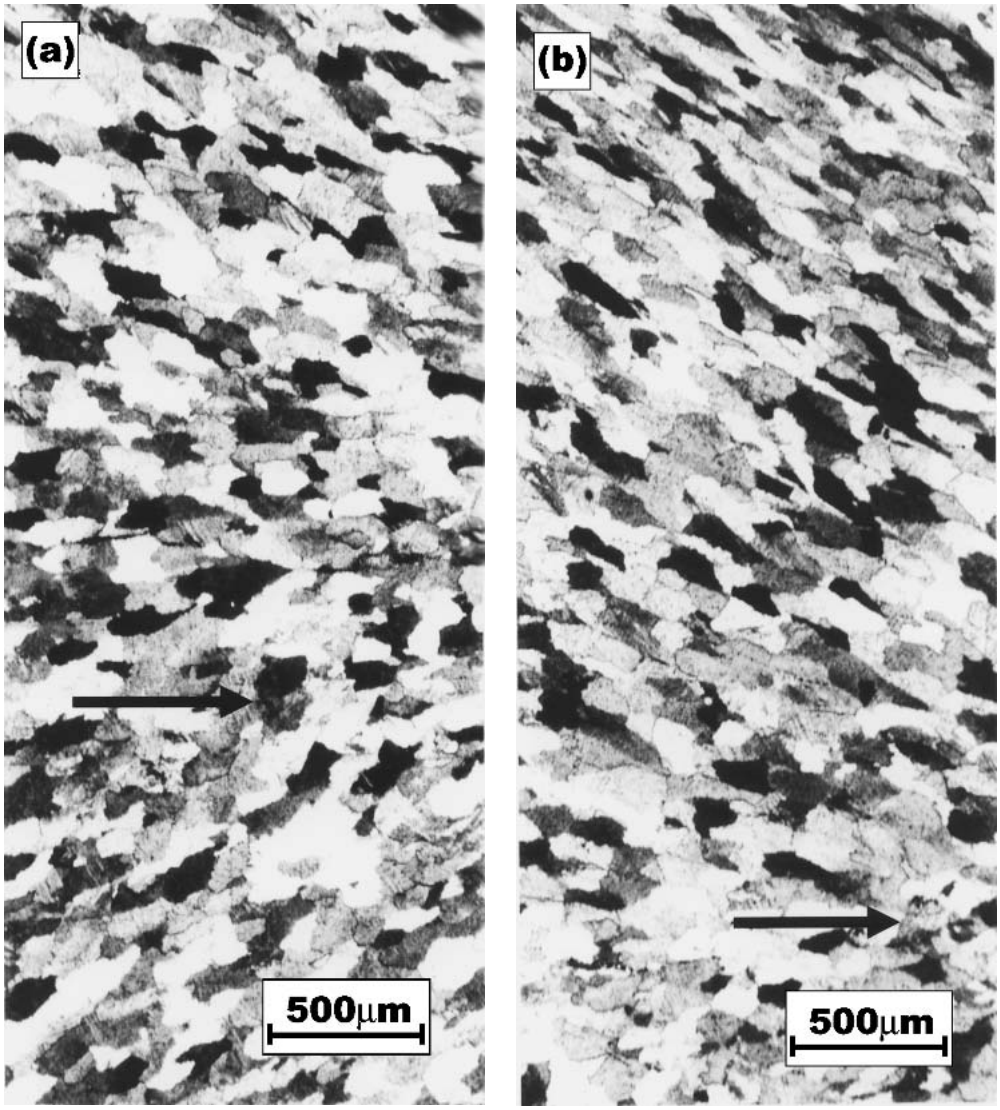


**Fig. 1** **(a)** Optical micrograph of the cross section of the TRC sheet. The material displays a characteristic columnar structure, which grows at approximately at 45° from the surface to the centerline of the coil; **(b)** columnar structure near the surface of the sheet showing the significant elongation of the grains and the progressive change in orientation from surface to center. The arrows in both pictures indicate the roll casting direction.

any intermediate annealing time or the strength of the aggregate and $S_f$ the UTS after sufficiently long annealing times have taken place, such that no more changes are observed if annealing is continued. The recrystallized fraction, $X_v$, was determined by correcting the fraction restored by recovery effects, which was carried out taking into consideration the time at which the first signs of recrystallization were observed metallographically.

If $S_0'$ represents the UTS of the material when the recrystallization process starts, then $X_v$ can be simply obtained by replacing $S_0$ in Eq 4 by $S_0'$. Figure 3 illustrates the change in the recrystallized fraction as a function of annealing time for the samples deformed to a different extent, annealed under non-isothermal conditions. The solid lines represent the description of the experimental data points by the model advanced by Semiatin et al,[3] whereas the dotted lines represent the description provided by the model advanced by Puchi et al.[1,2] As it can be appreciated, the results obtained by the application of both models for the description of the experimental data are practically undistinguishable from each other and provide a satisfactory characterization of the non-isothermal transformation.

However, the determination of the constants involved in the JMAK equation, including the apparent activation energy for recrystallization, can be carried out more readily if both models are used together. As has been pointed out above, the JMAK equation, commonly used for the description the change in the recrystallized fraction with annealing time under isothermal conditions, is usually expressed as:

$$X_v = 1 - \exp(-kt^n) = 1 - \exp\left[-0.693\left(\frac{t}{t_{0.5}}\right)^n\right] \qquad \text{(Eq 5)}$$

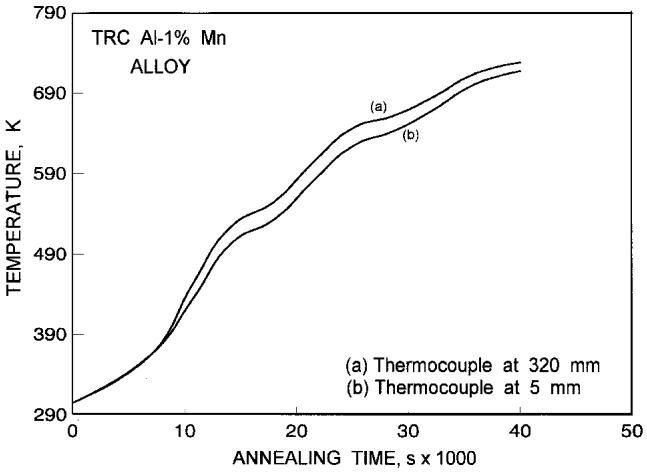


**Fig. 2** Temperature-time profile of a 3003 aluminum alloy during its annealing after cold rolling. Two thermocouples were inserted at 5 and 320 mm from the steel mandrel located at the center of the coil.

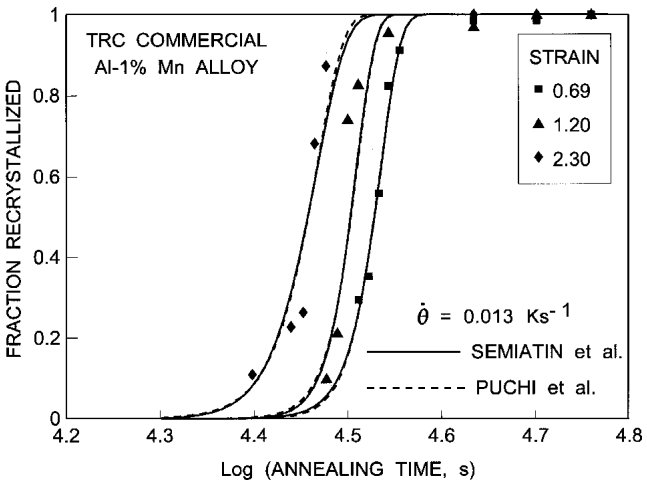


**Fig. 3** Change in the recrystallized fraction with annealing time, under non-isothermal conditions

where k and n represent the Avrami constants and t the annealing time. Furthermore, if it is assumed that the $t_{0.5}$ follows an Arrhenius equation of the form:

$$t_{0.5} = A \exp\left(\frac{Q_R}{RT}\right) \quad \text{(Eq 6)}$$

Equation 5 can be modified as:

$$X_v = 1 - \exp\left\{-B\left[\frac{t}{\exp\left(Q_R/RT\right)}\right]^n\right\} \quad \text{(Eq 7)}$$

In the above equations, A and B are constants, and the other parameters have already been defined. According to the model advanced by Puchi et al.,[1,2] if the annealing process is carried out at a constant heating rate, $\dot{\theta}$, the annealing period can be divided into a large number of small intervals, N, and the above equation would be given by:

$$X_v = 1 - \exp\left\{-B\left[\sum_{i=1}^{N} \delta t_i \exp\left(-\frac{Q_R}{RT_i}\right)\right]^n\right\} \quad \text{(Eq 8)}$$

where:

$$T_i = \theta\, t_i \quad \text{(Eq 9)}$$

The constants $Q_R$, B, and n in Eq 8 can be readily determined by non-linear regression analysis, by defining an objective function of the form:

$$\varphi = \sum_{i=1}^{N_E} \{X_{vi} - \hat{X}_{vi}\}^2 \quad \text{(Eq 10)}$$

and solving simultaneously the system of equations that results from the minimization condition:

$$\frac{\partial \varphi}{\partial B} = 0;\ \frac{\partial \varphi}{\partial Q_R} = 0;\ \frac{\partial \varphi}{\partial n} = 0 \quad \text{(Eq 11)}$$

although multiple solutions can be obtained depending upon the search interval for $Q_R$. In Eq 10, $N_E$ represents the number of experimental measurements of the volume fraction recrystallized, $X_{Vi}$, as a function of annealing time, and $\hat{X}_{Vi}$ the predictions of such a fraction by means of Eq 8.

On the other hand, from the expression proposed by Semiatin et al.[3] for the description of the change in the volume fraction recrystallized as a function of temperature during non-isothermal annealing, Eq 2, it is possible to define a different objective function from which, by linear regression analysis, a unique value of $Q_R$ can be determined. However, no direct information about the constants B and n present in such an equation would be obtained, unless different annealing experiments were conducted at different heating rates.

Therefore, this model can be used to compute an initial approximate value of $Q_R$ and the Puchi et al. model can then be subsequently used by defining the precise search interval for this constant, with the advantage that the two Avrami constants are simultaneously computed with the apparent activation energy for recrystallization. Table 1 summarizes the value of the numerical constants that were calculated in this way from the experimental data shown in Fig. 3.

One of the most striking features of the present results is the low value of the apparent activation energy for recrystallization

**Table 1 Computed Values of the Constants in Eq 8**

| Effective Strain | Semiatin et al. Model | Puchi et al. Model | | |
|---|---|---|---|---|
| | $Q_R$, kJmol$^{-1}$ | $Q_R$, kJmol$^{-1}$ | B | n |
| 0.693 | 70.8 | 69.3 | $1.06 \times 10^{3}$ | 2.65 |
| 1.204 | 72.2 | 78.5 | $1.29 \times 10^{5}$ | 2.50 |
| 2.303 | 39.8 | 33.5 | $2.61 \times 10^{-5}$ | 3.55 |

that are determined with both models, which are much lower than the activation energy for self-diffusion of aluminum and its alloys which has been reported to be approximately 142-156 kJ/mol, and the relatively high values of the Avrami exponent, n, that are also calculated. In the current study, the material was cold rolled at laboratory scale to effective strains in the range of approximately 0.7-2.3, conditions under which large second phase particles will play a fundamental role in the formation of the recrystallization nuclei.[11] Therefore, it would be expected that the nucleation of the recrystallized grains occurred by site saturation and that the kinetics of the transformation process were controlled mainly by growth. Accordingly, if such a process were controlled by bulk diffusion it would also be expected that the apparent activation energy for recrystallization were of the same order of magnitude as the activation energy for self-diffusion.

The present results indicate that for effective strains of the order of 0.70-1.20, the apparent activation energy for recrystallization is in the range of 70-80 kJ/mol, with Avrami exponents of approximately 2.50-2.70. However, as the effective strain applied to the material increases to about 2.30, the apparent activation energy for recrystallization decreases even further to values of 33-40 kJ/mol, and the Avrami exponent is found to increase to approximately 3.6. The analysis of the recrystallization data conducted by Semiatin et al.[3] for low carbon steel and a commercially purity titanium alloy indicated that the activation energies computed from their model were of the same order of magnitude as the activation energies for self-diffusion, $Q_S$, in these materials, which indicate the preponderance of bulk diffusion as the rate controlling process. In the case of mild steel, the value obtained was somewhat lower than $Q_S$, whereas in the titanium alloy it was somewhat higher, a result that was interpreted in terms of the solute atoms present in the alloy that could pin the grain boundaries during the recrystallization process. Also, the Avrami exponents found in this analysis were in the range of 0.7-1, which are in the lower end of the interval of 1-3 expected for this parameter according to Furu et al.[12]

The present results indicate that the strain applied to the material has a very important influence on the recrystallization kinetics, particularly when thickness reductions greater than 70% are applied to the material during cold rolling. For effective strains of less than approximately 1.2, the apparent activation energy for recrystallization is of the order of 0.5 $Q_S$ for this material and the Avrami exponents are maintained in the range pointed out previously, whereas for elevated applied strains this parameter is reduced up to approximately 0.25 $Q_S$ and the Avrami exponent is observed to increase above 3.5.

Thus, to corroborate these results and to determine if the data obtained from non-isothermal annealing experiments could give rise to anomalous values of the recrystallization parameters, a number of isothermal annealing experiments were conducted in the same material, in the temperature range of 623-723 K, employing only samples cold rolled to 50% thickness reduction. The results of these experiments are shown in Fig. 4, which are presented in terms of the restored fraction rather than the data corrected for recovery effects. The analysis of these data yielded a value for the apparent activation energy for recrystallization of approximately 34 kJ/mol and Avrami exponents near 1.

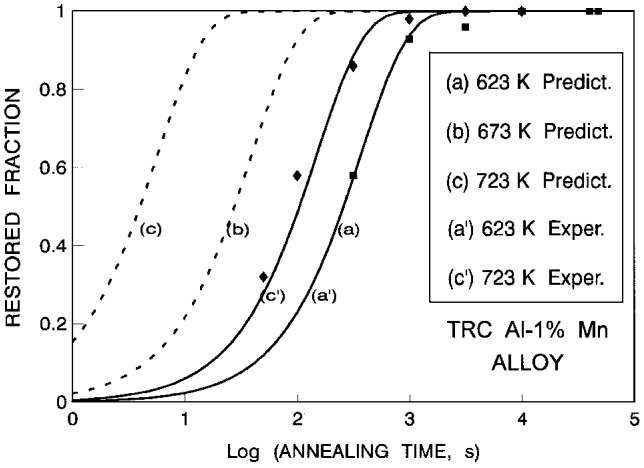


**Fig. 4** Change in the fraction restored with annealing time at 623, 673, and 723 K. The dotted lines indicate the predicted curves that are obtained by assuming activation energy for the restoration process of 156 kJ/mol.

Figure 4 shows, as solid lines, the location of the actual data determined experimentally and, as dotted lines, the location that such curves should have if the activation energy for restoration were identical to $Q_S$ for aluminum and its alloys. This figure clearly shows that if the activation energy for restoration were equal to $Q_S$ the location of the restoration curves in the diagram would have to be much wider than found experimentally. Even the predicted curves at 673 and 723 K, assuming that $Q_R = 156$ kJ/mol, are further apart than the experimental curves determined at 623 and 723 K. Therefore, such low values for $Q_R$ computed both from isothermal and non-isothermal data are indeed associated with the recrystallization process of the material and not with the non-isothermal models used for the description of the data themselves.

The reason of the existence of such relatively small values for $Q_R$ in the recrystallization of this TRC alloy is not at all clear. Its magnitude indicates that apparently the transformation of the deformed matrix into a new strain-free structure is carried out with less thermal energy than that required for self-diffusion and that by increasing the strain applied to the material the thermal energy needed to activate the recrystallization process can be decreased further.

As pointed out by Humphreys and Hatherly,[11] the migration of low and high angle grain boundaries represents a fundamental aspect of the transformation that takes place during the annealing of cold worked metals. The recovery stage as well as the nucleation of the recrystallized grains is affected significantly by the kinetics of low angle boundary mobility, whereas the growth of the nucleated grains is determined mainly by the mobility of high angle boundaries throughout the deformed matrix. Therefore, it could be possible that the low apparent activation energies for recrystallization determined in the present work for this alloy either during isothermal and non-isothermal annealing conditions were interpreted in terms of the activation energies associated with the mobility of low and high angle grain boundaries. If the migration of low angle grain boundaries required climb of edge dislocation segments in the boundary, it would be expected that this process was the

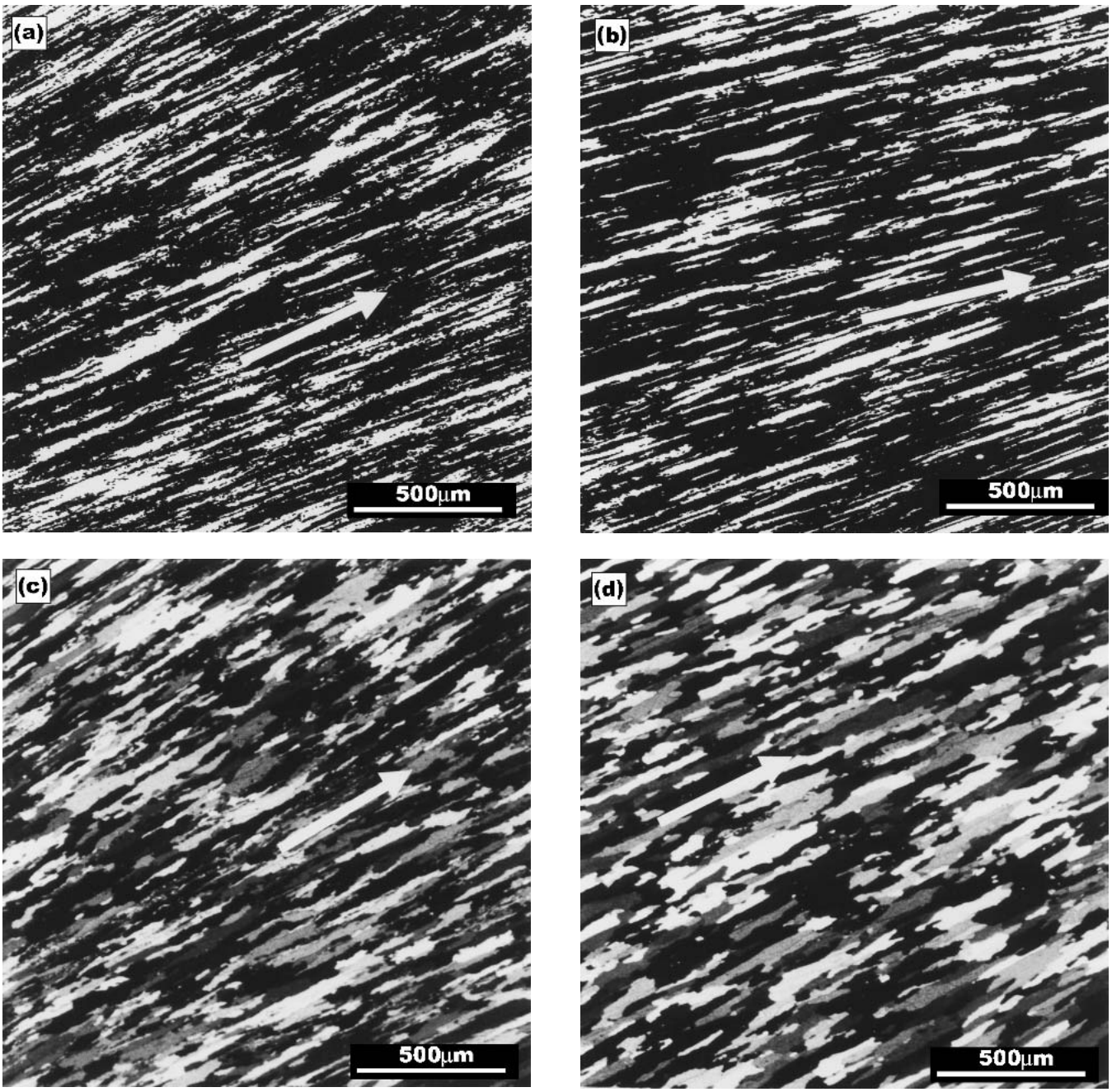


**Fig. 5** Optical photomicrographs showing the microstructural evolution of the samples cold rolled to an effective strain of 0.693 and annealed under non-isothermal conditions: **(a)** 498 K, **(b)** 564 K, **(c)** 754 K, and **(d)** 778 K. The arrows indicate the rolling direction.

rate controlling step and that the activation energy involved was close to that for self-diffusion. However, the work conducted by Ørsund and Nes[13] regarding the theory of mobility of low angle grain boundaries indicates that at low temperatures, such a process could also be controlled by pipe or core diffusion rather than climb. Therefore, the activation energy in this case would be different to $Q_S$. According to the work carried out by Murr[14] on aluminum, quoted by Humphreys and Hatherly,[11] the activation energies for core and boundary diffusion of this metal are approximately 82 and 84 kJ/mol, respectively, that is to say, almost half of the activation energy for self-diffusion. On the other hand, as far as the mobility of high angle grain boundaries in high purity metals is concerned, Humphreys and Hatherly[11] indicate that activation energies as low as 63-67 kJ/mol can be found in aluminum during recrystallization and capillary experiments, values even lower than those reported above for grain boundary diffusion. Therefore, it could be speculated that in the present case, although the presence of solute elements such as Mn, Fe, and Si gives rise to the existence of particles that could exert a significant effect in pinning the grain boundaries and retarding the recrystallization process, the alignment of such particles along the

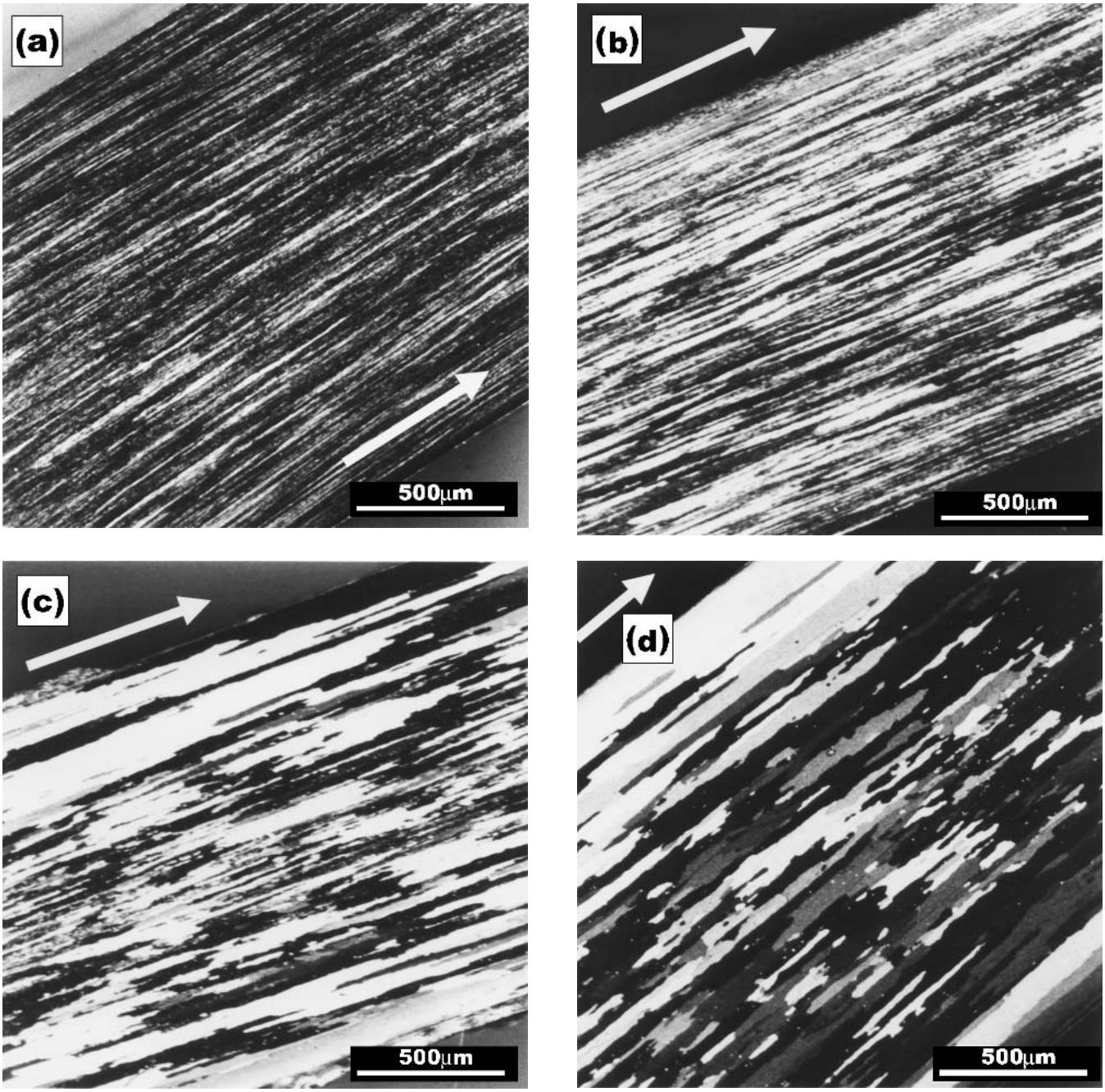


**Fig. 6** Optical photomicrographs showing the microstructural evolution of the samples cold rolled to an effective strain of 1.204 and annealed under non-isothermal conditions. **(a)** 498 K, **(b)** 710 K, **(c)** 718 K, and **(d)** 778 K. The arrows indicate the rolling direction.

rolling direction could restrict the mobility of the recrystallized grains in the ST direction. This would allow the migration of the high angle grain boundaries at a faster rate along the rolling direction, perhaps assisted by a grain boundary diffusion mechanism.

Such a hypothesis could have some support on the particular way in which recrystallization is conducted in TRC alloys (Fig. 5-7), which illustrate the recrystallization sequence of the samples deformed to a different extent and annealed under non-isothermal conditions. The photomicrographs presented in these figures clearly indicate that the recrystallization process in this alloy is characterized by a rapid growth of the recrystallized grains along the rolling direction. In contrast, the growth in the ST direction is relatively slow due to the pinning effect exerted by the second phase particles, which align themselves along the rolling direction.

Figure 5(a) and (b) illustrate that for the material deformed to an effective strain of 0.693, up to annealing temperatures of approximately 563 K, the microstructure remains virtually unchanged in comparison with that after cold rolling. In this case,

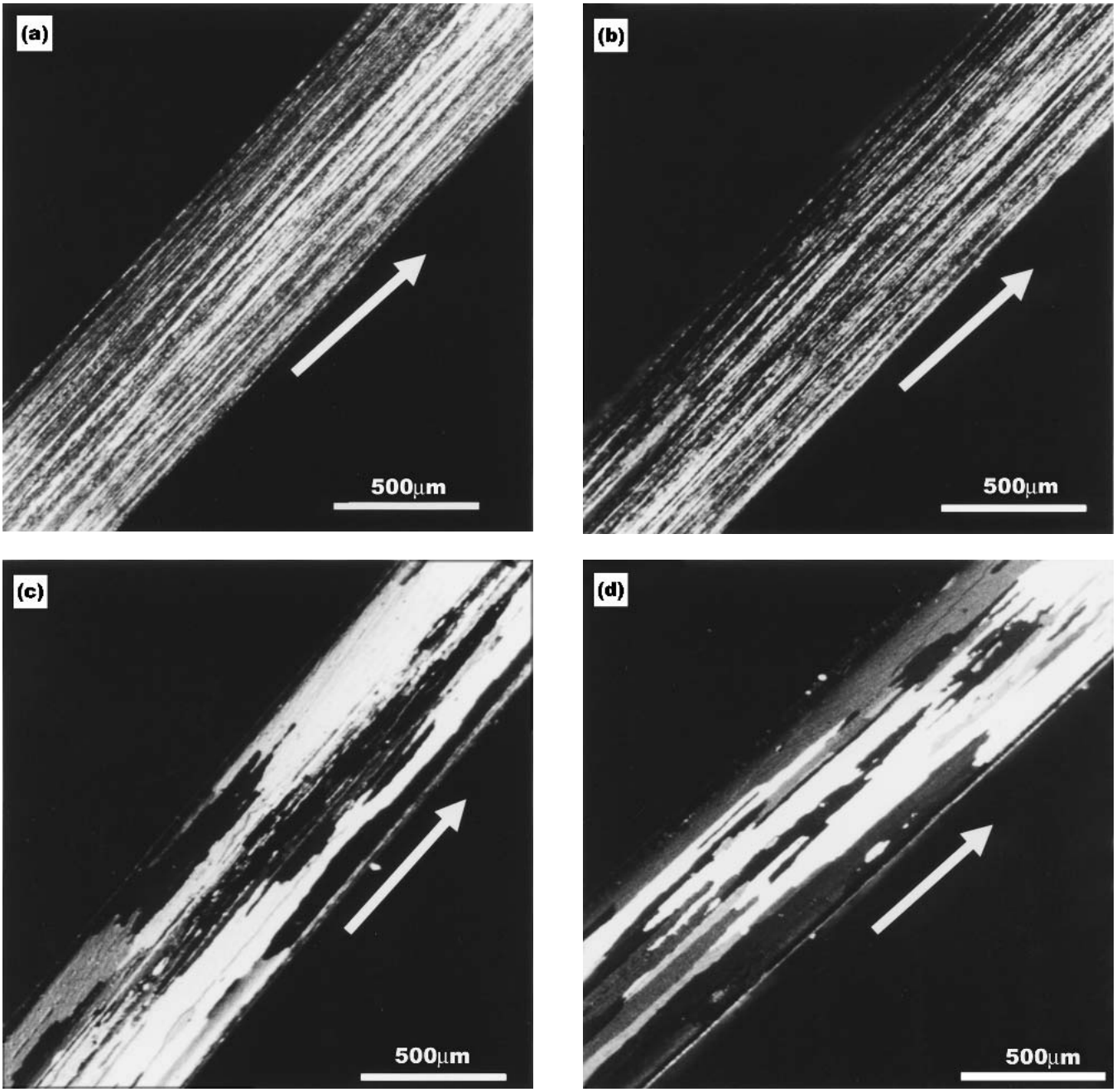


**Fig. 7** Optical photomicrographs showing the microstructural evolution of the samples cold rolled to an effective strain of 2.303 and annealed under non-isothermal conditions: **(a)** 498 K, **(b)** 676 K, **(c)** 688 K, and **(d)** 778 K. The arrows indicate the rolling direction.

the metallographic technique does not clearly define the grain boundaries, in contrast to the much better definition achieved after recrystallization is well advanced (Fig. 5c), when the material has reached an annealing temperature of approximately 753 K. After 14 h of annealing, when the temperature of the stock is 778 K, the structure still presents an elongated morphology which indicates that the rate of growth along the rolling direction (R), shown by the arrow, is much faster than that along the ST direction.

Figure 6(a) and (b), on the other hand, illustrate that as the effective strain applied to the material increases to approximately 1.2, the pattern is similar. At an annealing temperature of 498 K the structure still appears to be heavily deformed, with a poor definition of the grain boundaries. However, as the temperature increases to 710 K, the recrystallization process begins and a marked change in the microstructure of the alloy is produced (Fig. 6b). At a later stage, when the annealing temperature is about 718 K, the recrystallization process is observed to be much more advanced, particularly in those areas close to the surface of the sheet.

In the regions near the middle of the sample the recrystallized grains are much smaller, which indicates that in these

areas the recrystallization process is more difficult to accomplish. Such a result can be interpreted in terms of two phenomena related to the solute segregation during the solidification process, which progresses from the surface to the center of the sheet, leading eventually to the formation of the segregation plane. On one hand, it would be expected that the amount of solute elements in the matrix increased towards the center of the sheet and that the recrystallization kinetics in this region would be slowed down. On the other hand, the existence of a smaller number of large particles closer to the surface than the center of the sheet would give rise to a smaller number of recrystallization nuclei at the surface compared with the center. Figure 6(d), taken after 14 h of annealing, clearly shows a wide spectrum of grains sizes ranging from large grains at the surface, associated with a small number of recrystallization nuclei growing at a fast rate, to smaller grains at the center associated with a large number of nuclei growing a slow rate.

Regarding the material deformed to an effective strain of 2.3, Fig. 7(a-d) illustrate a similar pattern to the one described earlier. After approximately 10 h of annealing when the temperature of the stock reaches about 688 K (Fig. 7c), large recrystallized areas near the surface can be observed, together with some regions along the center which are still unrecrystallized. Such a recrystallization sequence leads to very heterogeneous distribution in grain sizes after long annealing periods (Fig. 7d). Furthermore, Fig. 5(a)-7(d) show that the difference in the growth rate along the R and ST directions leads to a recrystallized grain structure with an aspect ratio much greater than 1, a value that would be obtained for an equiaxed structure.

In an attempt to characterize the effect of the strain applied to the material on the recrystallization kinetics, Fig. 7 illustrates the change in the time required for 50% recrystallization as a function of the effective strain imposed by cold rolling. As it would be expected, as the strain applied to the material increases the time to achieve 50% recrystallization decreases and the recrystallization curve is displaced towards the left of the graph (Fig. 3). The change in $t_{0.5}$ with the effective strain can be best described by a simple parametric relationship of the form:

$$t_{0.5} = k_1 - k_2\,\varepsilon^m,\ s \qquad \text{(Eq 12)}$$

where $k_1 = 38815$, $k_2 = 6238.7$, and $m = 0.58$. The above expression can be combined with Eq 8 through the constant B, to describe the change in the recrystallized fraction with annealing time or current annealing temperature and effective strain. Equation 12 differs slightly from the parametric relationship usually used for the characterization of this kind of data, of the form:

$$t_{0.5} = k_3\,\varepsilon^{-p},\ s \qquad \text{(Eq 13)}$$

Previous investigations conducted on the same alloy have shown that, in the latter case, $p = 2.1$.[10] However, Eq 12 is quite satisfactory for such a purpose (Fig. 8).

In the current study, it has been possible to evaluate the effect of the strain applied to the material on the recrystallization kinetics in a wider range of effective strains than those previously applied when the investigation is conducted isothermally. In the latter case, as well as during non-isothermal annealing, the lower bound of the strain range is limited by the interaction that is established between the recrystallization and the precipitation processes characteristic of these types of alloys in which a large amount of solute elements remain in solution after casting. Also, the upper bound of such a range will be limited by the increase in the recrystallization kinetics as a result of the larger stored energy, which hinders the evaluation of the volume fraction recrystallized under isothermal conditions but not under non-isothermal annealing.

## 4. Conclusions

The recrystallization behavior of a cold rolled twin roll cast, commercial 3003 aluminum alloy under non-isothermal conditions, can be satisfactorily modeled by combining the approaches developed by Semiatin et al.[3] and Puchi et al.[1,2] The first approach allows the determination of the apparent activation energy for recrystallization without any ambiguity. This information can then be used in the second approach to define clearly the search range for $Q_R$ and to determine simultaneously this parameter and the Avrami constants, from experiments conducted at a single heating rate. In this way, it has been determined that $Q_R$ for this material varies between approximately 34-79 kJ/mol, with the trend being to find smaller values of this parameter as the strain applied to the material increases. Such low values of $Q_R$ were corroborated by iso-

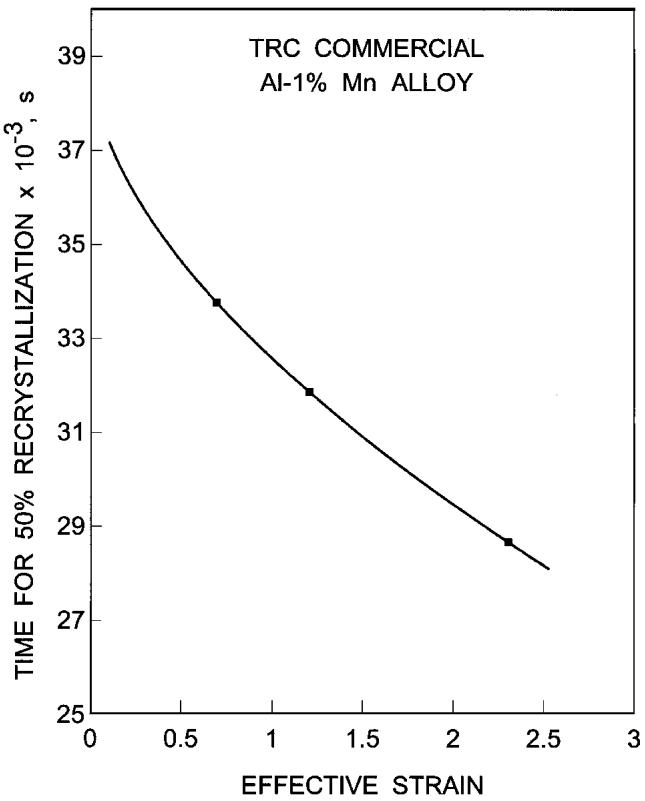


**Fig. 8** Change in the time for 50% recrystallization as a function of the strain applied

thermal experiments conducted in samples of the same material. The microstructural evolution of the samples annealed under non-isothermal conditions indicates that the rate of growth of the recrystallized grains in the rolling direction is significantly higher that in the ST direction, due to the pinning effect of the second phase particles aligned along the rolling direction, leading to recrystallized structures with an aspect ratio significantly higher than 1. The effect of the strain applied to the material on the recrystallization kinetics can be quantified precisely by expressing the time required to achieve a given recrystallized fraction as a function of the effective strain, by a simple parametric relationship that involves three numerical constants. Recrystallization experiments conducted under non-isothermal conditions are more suitable for the evaluation of the effect of the strain applied on the recrystallization kinetics in comparison with isothermal tests, since larger strains can be applied to material before the annealing treatment.

## Acknowledgments

This investigation has been conducted with the financial support of the Venezuelan National Fund for Science, Technology and Innovation (FONACIT) through project S1-2000000642, and of the Scientific and Humanistic Development Council of the Universidad Central de Venezuela (CDCH-UCV) through projects PI 08-17-2779-2000 and PG 08-17-4595-2000. The authors also acknowledge the collaboration of Mr. L. Peña and G. Di Lago in conducting some of the experimental work.

## References

1. E.S. Puchi, C. Villalobos, and A. Piñeiro: "Modeling Microstructural Evolution of Commercial Twin Roll Cast Aluminium-Iron-Silicon Alloys During Annealing Processes at Industrial Scale" in *Numerical Predictions in Deformation Processes on the Behavior of Real Materials,* S.I. Andersen, J.B. Bilde-Sørensen, T. Lorentzen, O.B. Pedersen, and N.J. Sørensen, ed., Risø National Laboratory, Roskilde, Denmark, 1994, pp. 276-81.
2. E.S. Puchi Cabrera, C. Villalobos, A. Carrillo, F. Di Simone, and P. Rodríguez: "Recrystallization of Cold Rolled Commercial Twin-Roll Cast Aluminium Alloys Under Non-Isothermal Conditions," *Proc. IV Int. Conf. on Recrystallization and Related Phenomena,* T. Sakai and H.G. Suzuki, ed., The Japan Inst. Metals, 1999, pp. 815-20.
3. S.L. Semiatin, I.M. Sukonnik, and V. Seetharaman: "An Analysis of Static Recrystallization During Continuous, Rapid Heat Treatment," *Metall. Mater. Trans.,* 1996, *27A*, pp. 2051-53.
4. V. Erukhimovitch and J. Baram: "Discussion of: An Analysis of Static Recrystallization During Continuous Rapid Heat Treatment," *Metall. Mater. Trans.,* 1997, *28A,* p. 2763.
5. D.W. Henderson: "Thermal Analysis of Non-Isothermal Crystallization Kinetics in Glass Forming Liquids," *J. Non-Crystalline Solids,* 1979, *30,* p. 301.
6. J.W. Cahn: "The Kinetics of Grain Boundary Nucleated Reactions," *Acta Metall.,* 1956, *4,* p. 449.
7. J.W. Cahn: "Transformation Kinetics During Continuous Cooling," *Acta Metall.,* 1956, *4,* p. 572
8. K. Matusita, T. Komatsu, and R. Yokota: "Kinetics of Non-Isothermal Crystallization Process and Activation Energy for Crystal Growth in Amorphous Materials," *J. Mater. Sci.,* 1984, *19,* p. 291.
9. S.L. Semiatin, I.M. Sukonnik, and V. Seetharaman: "Discussion of: An Analysis of Static Recrystallization During Continuous Rapid Heat Treatment, Author's Reply," *Metall. Mater. Trans.,* 1997, *28A*, p. 2764.
10. A. Olguín-Sandoval and E.S. Puchi-Cabrera: "Recrystallization Behavior of a Twin Roll Cast Commercial Aluminium-1% Manganese Alloy After Cold Rolling," *Mater. Sci. Technol.,* 2002, *18,* p. 81.
11. F.J. Humphreys and M. Hatherly: *Recrystallization and Related Annealing Phenomena,* 1st ed., Pergamon Press, 1996.
12. T. Furu, K. Marthinsen, and E. Nes: "Modeling Recrystallization," *Mater. Sci. Technol.,* 1990, *6,* p. 1093.
13. R. Ørsund, J. Hjelen, and E. Nes: "Local Lattice Curvature and Deformation Heterogeneities in Heavily Deformed Aluminum," *Scripta Metall.,* 1989, *23,* p. 1193.
14. L.E. Murr: *Interfacial Phenomena in Metals and Alloys,* Addison-Wesley, Reading, UK, 1975.